

Confinement effects on the spatial extent of the reaction front in ultrathin chemically amplified photoresists

Darío L. Goldfarb^{a)} and Marie Angelopoulos
IBM T. J. Watson Research Center, Yorktown Heights, New York 10598

Eric K. Lin, Ronald L. Jones, Christopher L. Soles, Joseph L. Lenhart, and Wen-li Wu
National Institute of Standards and Technology, Gaithersburg, Maryland 20899

(Received 1 June 2001; accepted 8 October 2001)

Sub-100 nm lithography poses strict requirements on photoresist material properties and processing conditions to achieve necessary critical dimension control of patterned structures. As resist thickness and feature linewidth decrease, fundamental materials properties of the confined resist polymer can deviate from bulk values and impact important processing parameters such as the postexposure bake (PEB) temperature. The effects of these confinement-induced deviations on image or linewidth spread have not been explored. In this work, we characterize the resist thickness dependence of the spatial extent of the reaction-diffusion process in a chemically amplified photoresist system under varying processing conditions. Bilayer samples are prepared with a lower layer of a protected polymer (*p-tert*-butoxycarboxystyrene) and a top layer of a de-protected polymer [poly(4-hydroxystyrene)] loaded with a photoacid generator. After flood exposure, PEB, and development, changes in the thickness of the protected polymer provide a measure of the spatial extent of the reaction front between the polymer layers. The velocity of the reaction front is significantly reduced with decreasing thickness of the protected polymer layer under identical processing conditions. © 2001 American Vacuum Society. [DOI: 10.1116/1.1421559]

I. INTRODUCTION

During photolithographic patterning of chemically amplified resists, factors such as photogenerated acid diffusion strongly affect the interface between protected and deprotected polymers as a function of bake time and temperature. The resolution limits of chemically amplified photoresists are affected by the material properties that control these factors and can result in either pattern blur or image spread. The constant demand for smaller device dimensions and thinner photoresist layers in the semiconductor industry introduces continuing challenges in the research arena. Critical dimension control of less than 10 nm will be required for structural dimensions below 100 nm. At these length scales, many properties of polymeric systems such as the glass transition temperature or the Young's modulus become significantly altered from their bulk quantities. The characterization and the fundamental understanding of these changes and their effect on feature resolution are essential for the development of new resist materials with the required sensitivity and/or resolution.

The diffusion of photogenerated acid (PGA) in the photoresist is among the most prominent factors identified in the literature as a source of image blur and dimensional control. There has been extensive past work on acid diffusion in chemically amplified resists using techniques such as ion conductivity,¹⁻⁸ diffusional lengths,⁹⁻¹³ spectrofluorometric detection,¹⁴⁻¹⁶ and computation methods.^{17,18} In general, these studies have used a simple interpretation of the chem-

istry and physics of the acid diffusion process, but a full description of the process involves a complex coupling of both reaction and diffusion processes.¹⁸ For example, each acid species catalyzes the deprotection reaction of a large number of protection groups increasing the effective range of a photogenerated acid. Acid diffusion is also a function of the local composition, which is in turn locally determined by the rate of reaction. Many other factors can contribute to image blur, including thermal de-protection where the deprotection occurs solely due to thermal fluctuations, disparities in the glass transition temperatures of the polymer species, as well as the presence of residual solvents and other impurities.

Many of the properties affecting the spatial extent of the de-protection reaction are known to be dependent on the dimensions of the feature. For example, the glass transition temperature, T_g , of ultrathin polymer films has been observed by many groups to increase or decrease with film thickness with a dependence upon the nature of the interaction between the polymer and the substrate.¹⁹ Other studies of thin films have demonstrated changes in small molecular probe diffusivity,²⁰ solvent absorption,²¹ and polymer chain mobility near surfaces and interfaces.^{22,23} Changes in the thermophysical properties of a resist polymer suggest changes in the dynamics of the material in confined geometries that directly impact critical photoresist processes such as acid diffusion during postexposure bake PEB.²⁴ The effect of film thickness on the spatial extent of the reaction front has been identified in past work, but has not been studied in detail. Fryer *et al.* report a reduced heat of reaction of the de-protection reaction in thin photoresist films using a local

^{a)}Author to whom correspondence should be addressed; electronic mail: goldfarb@us.ibm.com

thermal probe technique.¹¹ Houle *et al.* have also reported increases in the de-protection kinetics for thinner photoresist films.¹⁸

In this article, the spatial extent of the de-protection reaction is investigated in sub-100 nm films over length scales relevant to lithographic resolution (0–20 nm). We introduce a variation of a diffusional length technique using a bilayer sample prepared by spin coating a film of de-protected polymer loaded with a photoacid generator PAG on top of an ultrathin protected polymer layer. The bilayer system emulates the interface between exposed and unexposed regions in a patterned photoresist. In this simplified approach, a flood exposure removes the contribution of the aerial image to the spatial distribution of acid in the resist, and the remaining factors that modulate the spatial extent of de-protection events are exclusively materials related. During PEB, the acid may diffuse into the protected layer creating an advancing front of de-protection. After development, decreases in the thickness of the protected layer are used to identify the position of the boundary between protected and de-protected layers. By studying bilayer samples prepared under identical exposure and PEB conditions, any observed changes are related to confinement-induced effects from either the substrate or the confined polymer material.

II. EXPERIMENT

A. Materials

The de-protected polymer poly(4-hydroxystyrene) (PHOST) ($M_{r,n} = 5260$, polydispersity = 1.12 as measured by GPC) was obtained from Triquest.²⁵ Fully protected polymer *p*-tert-butoxycarboxystyrene (PBOCST) ($M_{r,n} = 15288$, polydispersity = 2.71) was prepared by free radical polymerization of *t*-butyl 4-vinylphenyl carbonate (Aldrich) following a literature procedure.²⁶ Di(*t*-butylphenyl) iodonium perfluorooctanesulfonate (PFOS) acid was obtained from DayChem. Propylene glycol methyl ether acetate (PGMEA) and 1-butanol were purchased from Aldrich. Developer CD-26 (TMAH 0.26 N) was obtained from Shipley.

B. Instrumentation

Film thickness was measured using an n&k analyzer (n&k Technology, Inc.). The interference fringes from the acquired UV-visible reflectivity spectrum were fit to the Forouhi–Bloomer equations. The film thickness calculated with this technique was compared with the values obtained using a variable angle spectroscopic ellipsometer (J. A. Woollam VASE). Only small systematic differences up to a maximum of 10 Å were detected between the two methods. Roughness was determined using an atomic force microscope (DI 3000 AFM, Digital Instruments) in tapping mode using standard DI software. Differential scanning calorimetry (DSC) (TA 2020 MDSC, TA Instruments) was used to obtain the glass transition temperature (T_g) of bulk samples. DSC measurements were performed using heating/cooling cycles at 10 °C/min with the experimental value of T_g determined in the second cycle.

C. Sample processing

Samples consisted of bilayers of protected (PBOCST) and de-protected (PHOST) polymers as the bottom and top layers, respectively, on a hydrophobic silicon substrate. Silicon wafers were pretreated by immersion in a solution of concentrated sulfuric acid (96%) and hydrogen peroxide (30%) in a 70:30 volume ratio at 56 °C for 1 h followed by rinsing with de-ionized water to remove any trace organic impurities from the substrate. A hydrophobic surface was generated by treating the silicon wafers with hexamethyldisilazane vapor prime in a vacuum oven (Yield Engineering Systems). The bottom PBOCST layer was spin cast from solution in PGMEA at 3000 rpm and subsequently baked at 130 °C for 60 s on a contact hot plate (1100 CEE, Cost Effective Equipment) and the film thickness determined. The top PHOST layer was spin cast on the PBOCST layer from a 1-butanol solution with a solids mass fraction of 5% PFOS and the bilayer was again baked at 130 °C for 60 s.

Exposure of the bilayer system to broadband UV radiation (Oriol Instruments) deposited a dose of 1000 mJ/cm², as measured with a dose meter (PowerMax). The dose necessary to create enough acid to de-protect the PBOCST layer during PEB was chosen after performing separate experiments with single layers of fully protected PBOCST carrying similar PAG loads, which were exposed to increasing amounts of radiation and placed in contact with standard aqueous developer. The “dose to clear” value was used as the criterion to determine a range of useful doses.

After postexposure baking (PEB) the flood exposed bilayer films at selected temperatures and times, the PHOST top layer and the de-protected section of the PBOCST bottom layer were removed by immersion of the wafer in TMAH 0.26 N for 30 s, followed by a rinse with de-ionized water. The thickness of the remaining PBOCST layer was measured as described above.

III. RESULTS AND DISCUSSION

Figure 1 shows the change in thickness of the lower protected polymer layer, d_{dev} , as a function of baking time for a range of PEB temperatures. The observed changes in thickness of the remaining PBOCST layer are expected from the development of a broadening or moving interface between the two polymer layers due to the de-protection reaction. We note that the postdevelopment AFM measurements on the PBOCST layer yielded rms roughness values on the order of (5–8) Å. The roughness was significantly smaller than the overall thickness removed and does not contribute to any error in the thickness measurement. Although a distribution of de-protection fractions is expected through the bilayer interface, we reasonably assume that the developed interface is proportional to a critical de-protection fraction to analyze the data. As a result, any variation in the deprotection profile from changes in material or transport properties in the interfacial region will be observed from changes in the remaining PBOCST thickness. For the data in Fig. 1, the original thickness of the protected layers was chosen at d_{PBOCST}

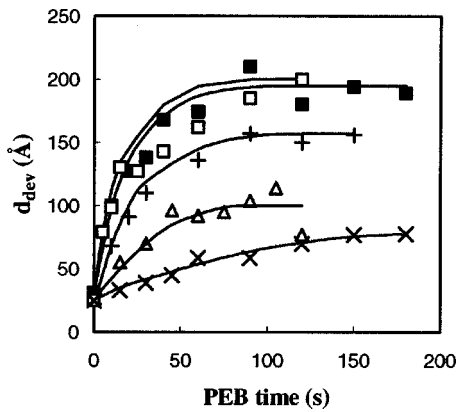


FIG. 1. Measured diffusional length (d_{dev}) of perfluorooctanesulfonic acid (PFOS) in PBOCST at different temperatures: (\times) 90 °C, (Δ) 100 °C, (+) 110 °C, (\square) 120 °C, (\blacksquare) 130 °C. Thickness: 1250 Å. The standard uncertainty in the d_{dev} measurement is ± 10 Å.

= 1250 Å. These samples will serve as a reference for those results obtained using thickness values below 1000 Å, which are presented later.

For all temperatures, increasing PEB time increases the rate at which the reaction front moves into the PBOCST layer as expected from an exposed PAG loaded PHOST layer next to a protected polymer layer. For each temperature, there is sharp rise in the rate at which the reaction front moves into the PBOCST layer that then reaches an apparent asymptotic limit at longer times. This more rapid initial rate of de-protection has been observed and analyzed in studies on similar systems.^{12,18} As the temperature increases, the rate at which the reaction front moves into the PBOCST layer increases. However, for PEB temperatures at or above the measured bulk PBOCST T_g (≈ 120 °C), the effect of the PEB temperature on the velocity of the reaction front is smaller than the error in the experiment. It is perhaps surprising that de-protection is observed at temperatures well below the T_g of PHOST ($T_g \approx 150$ °C) where the diffusivity of the acid has been found to be very low.^{12,18} Enhanced acid mobility at the interface between protected and de-protected layers at sub- T_g temperatures is possible resulting from a variety of factors including local changes in the T_g due to the presence of the PAG, residual casting solvent or a reduced T_g at the boundary. Nevertheless, the variations in the velocity of the reaction front with temperature strongly suggest that acid transport is determined by thermally activated events.

A systematic film loss of (20–30) Å in the bottom layer was detected after development on bilayers processed without PEB (Fig. 1, $t=0$). The same behavior was observed when unexposed films were developed, irrespective of the baking time. Rinsing of PBOCST films with 1-butanol led to the same thickness change, but repeated rinsing of the same PBOCST film with 1-butanol did not introduce any further loss. The systematic loss observed can be justified in terms of the molecular size and binding energy of the individual polymer chains. Removal of a loose monolayer of PBOCST from the surface by the casting solvent is possible due to a lower binding energy of those polymer chains compared to

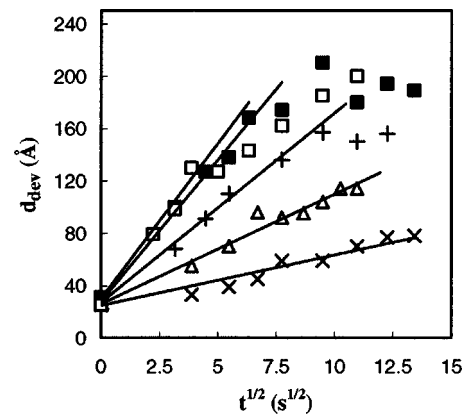


FIG. 2. Diffusion of PFOS into PBOCST at different temperatures. (\times) 90 °C, (Δ) 100 °C, (+) 110 °C, (\square) 120 °C, (\blacksquare) 130 °C. Thickness: 1250 Å. The standard uncertainty in the d_{dev} measurement is ± 10 Å.

the bulk film. A radius of gyration (R_g) of ~ 30 Å is expected for the $M_{r,n}$ of PBOCST used in our experiments which agrees with the observed thickness loss values.

As a simple approximation, we can analyze the movement of the reaction front into the PBOCST layer in terms of a Fickian-type model, namely $d_{\text{dev}} \propto t^{0.5}$, where t is time. For $T < T_{g,\text{PBOCST}}$ the movement of the reaction front is consistent with a Fickian-type scaling at short baking times (see Fig. 2). The velocity of the reaction front propagation can then be parametrized by an effective diffusion coefficient, D_{eff} . In earlier work, this diffusion coefficient was directly assigned to acid diffusion, but actually encompasses many other physical and chemical factors.

In relation to Fig. 2, the acid mobility at higher temperatures is large enough to preclude any quantification of its scaling prior to reaching a plateau. The source of the plateau is unknown at this time, however results from prior measurements of probe diffusion through PHOST below its T_g suggest that PAG diffusion in the PHOST layer is negligible and self-limiting reaction front propagation mechanisms have been proposed. These include the complex interplay of many factors including the coupling of diffusion with the chemical reaction, free volume generation in the reaction zone due to the evolution of gaseous reaction products, relaxation and densification of the de-protected layers and acid trapping in those de-protected regions with substantially slower chain dynamics. However, regardless of the exact combination of factors behind the movement of the reaction front, the dramatic slowdown of the boundary at longer bake times suggests that while this movement is finite, it occurs over significant distances under normal processing conditions.

We note that diffusion coefficients from the data in Fig. 2 are consistent with the values reported for other PGA in photoresists using a similar type of analysis. A comparison of diffusional lengths of several photoacids in polyhydroxystyrene-based matrices at different baking temperatures, obtained using experimental techniques, is given in Table I. A general close agreement with reported values for the diffusion of photoacids was obtained, given the variations in molecular size, and the wide range of processing

TABLE I. Reported diffusion coefficient of several photoacids under different temperature ranges. 24 BS: 2,4-dimethyl benzenesulfonic, PFBS: perfluorobutanesulfonic, PFOS: perfluorooctanesulfonic.

Photoacid	PBOCST (f_{prot})	Thickness (\AA)	PEB temp. ($^{\circ}\text{C}$)	D (cm^2/s)	Ref.
PFBS	1.0	12 000	65–105	5×10^{-16} – 1.5×10^{-13}	18
PFOS	1.0	1300	90–130	2.6×10^{-16} – 1.0×10^{-14}	This work
24 BS	0.36	7000	60–120	6×10^{-15} – 3×10^{-14}	3
PFBS	0.0	12 000	65–105	4×10^{-17} – 1×10^{-15}	18
PFBS	0.0	5000	165–185	3.3×10^{-14} – 5.4×10^{-12}	13

conditions. The low diffusion coefficients of long chain fluorinated PAGs are directly related to a relatively large molecular volume.²⁷ We also note that these values are comparable with the diffusion coefficients of linear iodoctane, comparable in size to PFOS, into a nonreactive matrix of glassy poly(styrene).²⁸ In addition, the activation energy obtained in this work for the diffusion of PFOS in a 1250 \AA layer of PBOCST between 90 and 110 $^{\circ}\text{C}$ ($E_a = 37 \pm 3$ kcal/mol) agrees with the reported E_a for the diffusion of perfluorobutanesulfonic acid PFBS in the same resist¹⁸ within the experimental error.

To explore the thickness dependence of the movement of the reaction front, a series of experiments were conducted at 110 $^{\circ}\text{C}$, just below $T_{g,\text{PBOCST}}$ for protected layer thicknesses ranging from 2000 to 375 \AA . The samples are prepared in identical fashion and any differences in the spatial extent of the reaction front arise from the reduced dimensions of the PBOCST layer. In Fig. 3, the changes in the thickness of the de-protected layer are plotted as a function of time in Fickian form. As the initial PBOCST film thickness decreases, the rate of propagation of the reaction front into the PBOCST layer is significantly reduced. Extending the use of the Fickian model, we can parametrize these changes through an effective rate coefficient, D_{eff} , from the slopes of the data in Fig. 3. D_{eff} values for the advance of the de-protection front were determined using a simplified mathematical approach

similar to that followed by Schlegel *et al.*⁹ The solution from Fick's laws to the infinite diffusion case was obtained²⁹:

$$C(x,t) = \frac{C_0}{2} \left[1 - \operatorname{erf} \left(\frac{x}{2(Dt)^{0.5}} \right) \right]. \quad (1)$$

After a certain baking time t the developer is able to remove a de-protected PBOCST layer up to a certain depth (d_{dev}) characterized by a given deprotection level f_{prot} , then $x = d_{\text{dev}}$. If we estimate that the local acid concentration at the surface of the developed PBOCST layer $C(d_{\text{dev}},t)$ is much smaller than the surface concentration C_0 and establish approximate upper and lower limits⁹

$$0.5 > 2C(d_{\text{dev}},t)/C_0 > 0.05. \quad (2)$$

Then, using Eq. (1),

$$0.8 < \frac{d_{\text{dev}}}{2(Dt)^{0.5}} < 1.6. \quad (3)$$

A good approximation to calculate the diffusion coefficients for the photoacid is

$$d_{\text{dev}} \approx 2.4(Dt)^{0.5}. \quad (4)$$

The extracted D_{eff} values are plotted as a function of the initial PBOCST thickness in Fig. 4. The coefficient shows an asymptotic limit for PBOCST layers thicker than 600 \AA but is dramatically reduced for protected layer thicknesses less than 600 \AA . The dramatic slowdown of the de-protection front indicates thickness dependence of one or more PBOCST polymer material properties that control the resolution limits of chemically amplified resists such as acid diffusion.

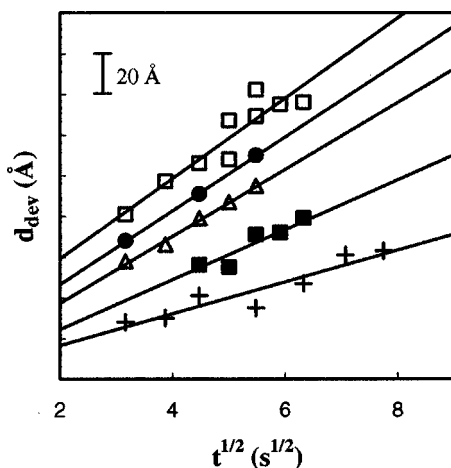


FIG. 3. Diffusion of PFOS into PBOCST at different thickness. (+) 375 \AA ; (■) 520 \AA ; (Δ) 610 \AA ; (●) 1250 \AA ; (□) 2000 \AA at 110 $^{\circ}\text{C}$. The data for each thickness are offset vertically for clarity. The standard uncertainty in the d_{dev} measurement is ± 10 \AA .

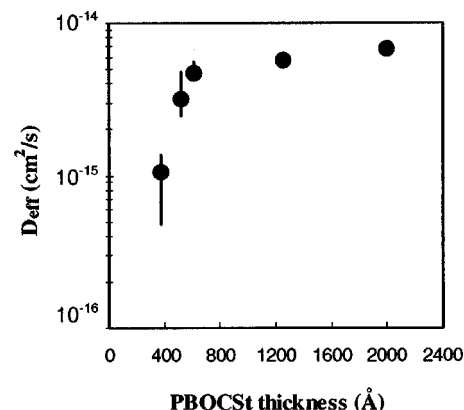


FIG. 4. D_{eff} as a function of film thickness for PFOS in PBOCST at 110 $^{\circ}\text{C}$.

These results are consistent with decreased heats of reaction in photoresist thin films loaded with PAG using the thermal probe studies of Fryer *et al.*¹¹

In the literature, there have been reports on changing transport properties of small molecules in ultrathin films. Probe diffusion studies in ultrathin supported polymer films reveal that transport coefficients can be affected by positive or negative deviations from bulk values, depending on the presence of a free interface, the chain affinity for the substrate and the nature of the polymer itself. The diffusion of small molecules in ultrathin polystyrene (PS), poly isobutyl methacrylate (PiBMA) and poly 2-vinylpyridine (P2VP) films using fluorescence nonradiative energy transfer was studied with a polymer bilayer configuration near the T_g .²⁰ The authors found that probe diffusion in PS films on fused quartz substrates *decreased* for a film thickness below ~ 1500 Å, but for PiBMA and P2VP no discernible changes in probe diffusion were found in ultrathin films compared to bulk. This behavior was attributed to chain packing and architecture, but specific polymer-substrate effects were discarded. Decoupling of these potential factors as well as the diffusion and reaction processes is complex and beyond the scope of this work, however we have clearly shown a thickness dependence of the de-protection front velocity that directly impacts resolution control of sub-100 nm patterns. These results show that the spatial extent of the reaction front between exposed and unexposed regions of a resist may be significantly slowed and therefore more controllable with PEB for $T < T_{g,prot}$, where $T_{g,prot}$ is the glass transition temperature of the protected polymer.

IV. CONCLUSION

A method that encompassed standard processing steps regularly found in the lithographic industry (coat, expose, bake, develop, measure thickness) was adopted to analyze the spatial extent of the reaction front, or line edge, between exposed (de-protected) and unexposed (protected) regions in resist materials. The de-protected polymer, containing the active acid groups, is glassy during baking while the protected polymer was examined both in the glassy and rubbery regimes. The glassy de-protected phase prohibits more than a finite amount of acid from diffusing into the protected phase, producing an asymptotic limit to the de-protection front as a function of bake time. For the case of a rubbery protected polymer, the velocity of the reaction front into the protected polymer layer is predictably faster and its rate is relatively independent of bake temperature. For a glassy protected phase, the rate is significantly reduced and is well approximated with a Fickian diffusion model at short baking times. In addition, the dependence of the rate on bake temperature indicates that the process has more controllability in this limit. Finally, the boundary migration rate is found to be a strong function of film thickness. For film thicknesses less

than 600 Å, the velocity of the reaction front is significantly reduced. The precise origin of this thickness dependence is still unclear, but is consistent with observation of reduced mobility of the small molecules or PGAs due to thickness dependent thermophysical properties of the protected polymer.

ACKNOWLEDGMENTS

The authors would like to thank David R. Medeiros for the synthesis of PBOCST and Rane W. Kwong for the GPC measurements. The authors also gratefully acknowledge DARPA for financial support under Contract No. N66001-00-C-8803. C. Soles and J. Lenhart gratefully acknowledge support from the NIST-National Research Council Postdoctoral Program.

- ¹J. Nakamura, H. Ban, K. Deguchi and A. Tanaka, *Jpn. J. Appl. Phys.*, Part 1 **30**, 2619 (1991).
- ²T. H. Fedynshyn, J. W. Thackeray, J. H. Georger, and M. D. Denison, *J. Vac. Sci. Technol. B* **12**, 3888 (1994).
- ³T. Itani, H. Yoshino, N. Fujimoto, and K. Kasama, *J. Vac. Sci. Technol. B* **14**, 3026 (1995).
- ⁴T. Itani, H. Yoshino, S. Hashimoto, M. Yamana, N. Samoto, and K. Kasama, *J. Vac. Sci. Technol. B* **14**, 4226 (1996).
- ⁵T. Itani, H. Yoshino, S. Hashimoto, M. Yamana, N. Samoto, and K. Kasama, *Jpn. J. Appl. Phys.*, Part 1 **35**, 6501 (1996).
- ⁶T. Itani, H. Yoshino, S. Hashimoto, M. Yamana, N. Samoto, and K. Kasama, *J. Vac. Sci. Technol. B* **15**, 2541 (1997).
- ⁷T. Itani, Y. Yoshino, S. Hashimoto, M. Yamana, N. Samoto, and K. Kasama, *Microelectron. Eng.* **35**, 149 (1997).
- ⁸T. Itani, S. Hashimoto, M. Yamana, N. Samoto, and K. Kasama, *Microelectron. Eng.* **41/42**, 363 (1998).
- ⁹L. Schlegel, T. Ueno, N. Hayashi, and T. Iwayanagi, *Jpn. J. Appl. Phys.*, Part 1 **30**, 3132 (1991).
- ¹⁰J.-B. Kim, J.-H. Choi, Y.-G. Kwon, M.-N. Hung, and K.-H. Chang, *Polymer* **40**, 1087 (1999).
- ¹¹D. S. Fryer, S. Bollepali, J. J. de Pablo, and P. F. Nealey, *J. Vac. Sci. Technol. B* **17**, 3351 (1999).
- ¹²S. V. Postnikov, M. D. Stewart, H. Vi Tran, M. A. Nierode, D. R. Medeiros, T. Cao, J. Byers, S. E. Webber, and C. G. Willson, *J. Vac. Sci. Technol. B* **17**, 3335 (1999).
- ¹³M. D. Stewart, M. H. Sommerwell, H. Vi Tran, S. V. Postnikov, and C. G. Willson, *Proc. SPIE* **3999**, 665 (2000).
- ¹⁴P. M. Dentinger, B. Lu, J. W. Taylor, S. J. Bukofsky, G. D. Feke, D. Hessman, and R. D. Grober, *J. Vac. Sci. Technol. B* **16**, 3767 (1998).
- ¹⁵B. Lu, J. W. Taylor, F. Cerrina, C. P. Soo, and A. J. Bourdillon, *J. Vac. Sci. Technol. B* **17**, 3345 (1999).
- ¹⁶E. Richter, S. Hien, and M. Sebald, *Microelectron. Eng.* **53**, 479 (2000).
- ¹⁷E. Croffie, M. Cheng, and A. Neureuther, *J. Vac. Sci. Technol. B* **17**, 3339 (1999).
- ¹⁸F. A. Houle, W. D. Hinsberg, M. Morrison, M. I. Sanchez, G. Wallraf, C. Larson, and J. Hoffnagle, *J. Vac. Sci. Technol. B* **18**, 1874 (2000).
- ¹⁹D. S. Fryer, P. F. Nealey, and J. J. de Pablo, *Macromolecules* **33**, 6439 (2000), and the references included therein.
- ²⁰D. B. Hall and J. M. Torkelson, *Macromolecules* **31**, 8817 (1998).
- ²¹K. E. Mueller, W. J. Koros, C. A. Mack, and C. G. Willson, *Proc. SPIE* **3049**, 706 (1997).
- ²²K. C. Tseng, N. J. Turro, and C. J. Durning, *Phys. Rev. E* **61**, 1800 (2000).
- ²³E. K. Lin, R. Kolb, S. K. Satija, and W. L. Wu, *Macromolecules* **32**, 3753 (1999).
- ²⁴C. L. Soles, E. K. Lin, J. L. Lenhart, R. L. Jones, W. L. Wu, D. L. Goldfarb, and M. Angelopoulos, *J. Vac. Sci. Technol. B* (accepted).
- ²⁵Certain commercial equipment and materials are identified in this article in order to specify adequately the experimental procedure. In no case does such identification imply recommendation by the National Institute of

Standards and Technology nor does it imply that the material or equipment identified is necessarily the best available for this purpose.

²⁶J. M. J. Fréchet, E. Eichler, H. Ito, and C. G. Willson, *Polymer* **24**, 995 (1983).

²⁷G. M. Wallraff, S. Bangsaruntip, N. Fender, W. Hinsberg, F. Houle, P.

Brock, J. Hoffnagle, M. Sanchez, C. E. Larson, G. Bretya, and W. Chau, *Proc. SPIE* 375 (2001).

²⁸T. P. Gall, R. C. Lasky, and E. J. Kramer, *Polymer* **31**, 1491 (1990).

²⁹J. S. Kirkaldy and D. J. Young, *Diffusion in the Condensed State* (The Institute of Metals, London, UK, 1985), p. 21.